Interpretation of the Hume-Rothery electron concentration rule in the T_2Zn_{11} (T=Ni, Pd, Co, and Fe) γ brasses based on first-principles FLAPW calculations

R. Asahi,[1] H. Sato,[2] T. Takeuchi,[3] and U. Mizutani[4,*]
[1]*Toyota Central R&D Laboratories, Inc., Nagakute, Aichi 480-1192, Japan*
[2]*Department of Physics, Aichi University of Education, Kariya-shi, Aichi 448-8542, Japan*
[3]*Ecotopia Science Institute, Nagoya University, Furo-cho, Chikusa-ku, Nagoya 464-8603, Japan*
[4]*Department of Crystalline Materials Science, Nagoya University, Furo-cho, Chikusa-ku, Nagoya 464-8603, Japan*
(Received 23 January 2005; revised manuscript received 5 July 2005; published 2 September 2005)

The first-principles full-potential augmented plane wave (FLAPW) band calculations were performed for a series of T_2Zn_{11} (T=Ni, Pd, Co, and Fe) γ brasses to elucidate the Hume-Rothery electron concentration rule. The pseudogap is found immediately below the Fermi level E_F in the Ni_2Zn_{11} and Pd_2Zn_{11} γ brasses. A resulting gain in the electronic energy is attributed to their stabilization in the same way as in Cu_5Zn_8 and Cu_9Al_4 previously studied. However, the pseudogap is essentially shifted above E_F in both Co_2Zn_{11} and Fe_2Zn_{11}. The Fourier analysis of the FLAPW wave function was made at the symmetry point N of the reduced Brillouin zone in the energy range involving the pseudogap. It is found that the plane wave giving rise to the largest Fourier component always resonates with the {330} and {411} zone planes to produce the pseudogap near E_F. Moreover, a single-branch energy dispersion relation was constructed in the extended zone scheme by averaging the wave vector $2(\mathbf{k}+\mathbf{G})$ having the largest Fourier component of the FLAPW wave function over selected electronic states in the Brillouin zone. The e/a value thus deduced is found to be close to $21/13=1.615$ for Cu_5Zn_8, Cu_9Al_4, Ni_2Zn_{11}, and Pd_2Zn_{11} γ brasses but to be only 1.4 and 1.3 for Co_2Zn_{11} and Fe_2Zn_{11}, respectively.

DOI: 10.1103/PhysRevB.72.125102 PACS number(s): 71.20.Gj, 81.30.Bx

I. INTRODUCTION

The γ brass has been known for many years as a structurally complex alloy phase containing 52 atoms in its cubic unit cell. Its structure determination dates back to 1926, when Bradley and Thewlis[1] identified the Cu-Zn γ brass as possessing the chemical formula Cu_5Zn_8 from their x-ray-diffraction studies. Westgren and Phragmén[2,3] pointed out in 1929 that Cu_5Zn_8 and Cu_9Al_4 are isostructural to each other and stabilized at the common electron per atom ratio $e/a=21/13$. Here the electron per atom ratio e/a in an alloy is conventionally defined as a weighted mean of valencies of constituent elements.

In 1931, Ekman[4] reported that the γ brass can be formed by dissolving different transition-metal elements T into either divalent Zn or Cd and revealed its formation in the Co-Zn, Fe-Zn, Ni-Zn, Pd-Zn, Rh-Zn, Pt-Zn, and Ni-Cd alloy systems. He pointed out that their formation ranges are centered at T_5Zn_{21} or 19.2 at.% T and concluded that transition-metal atoms apparently possess a vanishing valency, provided that the valency of Zn is 2 while the universal electron concentration equal to 21/13 is assigned to stabilize the γ-brass structure. Stimulated by these findings, in 1936 Mott and Jones[5] attempted to interpret why γ brasses are stabilized at the specific e/a value of 21/13 by assuming simultaneous contacts of the free-electron Fermi sphere with the set of {330} and {411} zone planes constructed from the strongest x-ray-diffraction line.

Research on the stabilization mechanism of a structurally complex alloy phase revived its interest after the discovery of a number of thermally stable quasicrystals and their approximants for the past two decades.[6,7] The pioneering work has been done by Fujiwara,[8] who revealed the pseudogap at the Fermi level E_F in the Al-Mn approximant containing 138 atoms in its cubic cell by performing the linearized muffin-tin orbital (LMTO) band calculations and pointed out that it contributes to lowering the electronic energy of the system. Since then, the pseudogap at E_F has been revealed both theoretically and experimentally in quasicrystals and their approximants without exception.[9–15] The formation of the pseudogap at E_F certainly results in partial depletion of electrons carrying the highest kinetic energies and, hence, is obviously the most effective to lower the electronic energy of a system. This would naturally contribute to the stability of such structurally complex alloy phases.

In the past decade, the LMTO studies on the theoretical side and spectroscopic studies on the experimental side have provided ample evidence for the presence of orbital hybridizations among constituent elements, which give rise to the pseudogap across E_F.[11,13,14] Although the role of orbital hybridizations in the formation of the pseudogap across E_F has been widely accepted, a clear-cut interpretation for the stability of such structurally complex alloy phases at specific electron concentration in conjunction with the Hume-Rothery electron concentration rule has not been provided in a straightforward manner from the LMTO band calculations.

The γ brass containing 52 atoms in its unit cell can be regarded as being typical of a structurally complex alloy phase and be treated in the FLAPW method within reasonable computing time. Indeed, Asahi *et al.*[16] performed the FLAPW band calculations for the Cu_5Zn_8 and Cu_9Al_4 γ brasses as a representative of the complex alloy phases to extract the Fermi surface–Brillouin zone interaction responsible for the formation of the pseudogap at E_F. This was

accomplished by calculating the $|\mathbf{G}|^2$ dependence of the Fourier coefficient in the plane-wave expansion of the FLAPW wave function in the region outside the muffin-tin potential for states near E_F, where $|\mathbf{G}|^2$ is the square of the reciprocal-lattice vector in the units of $(2\pi/a)^2$. They were led to the conclusion that electrons sustaining the pseudogap resonate with lattice planes associated with {330} and {411} zones and give rise to standing waves for both Cu_5Zn_8 and Cu_9Al_4 γ brasses. This clearly explained why these two compounds having different solute concentrations are stabilized at the same e/a value of $21/13=1.615$ and was taken as a demonstration of the Hume-Rothery electron concentration rule beyond the oversimplified free-electron model by Mott and Jones.[5]

According to the updated handbook of equilibrium phase diagrams,[17] γ brasses are formed in more than 20 binary alloy systems. Depending on a combination of constituent elements, they will naturally yield a variety of electronic structures. It is therefore surprising for all of them to crystallize into the same complex structure accommodating 52 atoms in the cubic cell in spite of the difference in an overall electronic structure. More important is that most γ brasses are not *a priori* known to possess the electron concentration equal to 21/13 as a magic number assigned to them. This is particularly true, when the transition-metal element is involved as a major component. For instance, Raynor[18] assigned negative valencies like −0.61, −1.71, −2.66, −3.66, and −4.66 to Ni, Co, Fe, Mn, and Cr, respectively, so as to bring the average electron concentration of $CrAl_7$, $MnAl_6$, Co_2Al_9, and $NiAl_3$ to a common value of 2.05–2.1, whereas a small positive valency was suggested to be more appropriate for T elements in the Cu-T alloys by Haworth and Hume-Rothery.[19] Based on the LMTO band calculations, Trambly de Laissardiére *et al.*[20] interpreted the possession of a negative valency for the T element in Al-T alloys in terms of an increase in *sp* electrons around the T atom rather than the charge transfer to the *d* orbitals assumed originally by Raynor.

We have performed the FLAPW band calculations for the T_2Zn_{11} (T=Ni, Pd, Co, and Fe) γ brasses and analyzed the Fourier spectrum of the FLAPW wave function sustaining the pseudogap at E_F. Special attention was directed to the following two aspects: (i) whether or not the electronic energy is gained by forming the pseudogap across the Fermi level, and (ii) whether or not the calculated e/a value can reproduce the empirical value of 21/13. The latter is evaluated by constructing the effective Fermi sphere under the approximation that the dominant FLAPW plane wave averaged over the Brillouin zone directly provides a single-branch dispersion relation in the extended zone scheme.

II. ELECTRONIC-STRUCTURE CALCULATIONS

In the present work, we chose Ni-Zn, Pd-Zn, Co-Zn, and Fe-Zn γ brasses from the literature.[17,21] All of them were reported to involve 52 atoms in the cubic unit cell with the space group of $I\bar{4}3m$ for Ni-Zn, Pd-Zn, and Fe-Zn γ brasses but that of $P\bar{4}3m$ for Co-Zn.[21] However, our structure analysis revealed that the Co-Zn γ brass is also identified to be

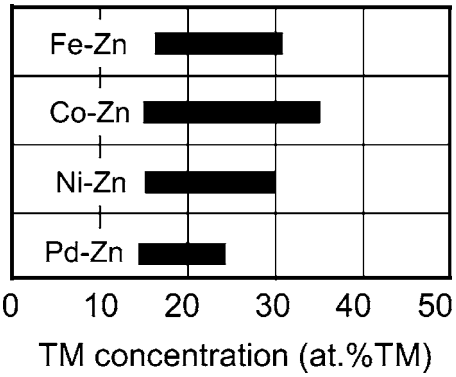

FIG. 1. γ-brass single-phase formation range in the T-Zn (T=Fe, Co, Ni, and Pd) alloy systems.

$I\bar{4}3m$.[22] Figure 1 shows the composition range where a single phase is formed for these four alloy systems. The maximum T concentration extends up to 35 at.% in the Co-Zn but only 25 at.% in the Pd-Zn system. It is, however, interesting to note that the minimum T concentration is about 15 at.% T, regardless of the atomic species of the T element involved.

The atomic structure of the γ brass with the space group $I\bar{4}3m$ can be described by locating the 26-atom cluster at the center and corner of the bcc lattice. The cluster consists of four atoms in the inner tetrahedral (IT) sites 8(c), four atoms in the outer tetrahedral (OT) sites 8(c), six atoms in the octahedral (OH) sites 12(e), and 12 atoms in the cubo-octahedral (CO) sites 24(g). All the data for the T-Zn (T=Ni, Pd, Fe) γ brasses available in the literature[23–25] are consistent with the preferential occupation of T atoms in the OT sites and Zn atoms in all remaining sites, though the chemical disorder inevitably exists in each site, depending on the composition chosen. For example, Brandon *et al.*[25] could synthesize a $Fe_{24}Zn_{76}$ γ-brass single crystal and determine its atomic structure by diffraction techniques. It was concluded that four Fe atoms are exclusively filled into the OT sites and the remaining two Fe atoms into IT sites sharing with two Zn atoms in the 26-atom cluster. Independently, we have carried out the Rietveld structure analysis for powder diffraction data taken on the $Co_{20}Zn_{80}$ γ brass at the SPring-8 Synchrotron radiation facility, Japan. The best refinement was achieved for the structure in which Co atoms enter more preferentially into the OT sites and Zn atoms into the IT sites.[22]

In the present band calculations, chemical disorder must be ignored. Hence, we chose the γ-brass structure with the space group $I\bar{4}3m$, in which OT sites are fully filled with T atoms whereas all remaining sites with Zn atoms. This leads to the chemical formula T_2Zn_{11} and corresponds to the minimum concentration of 15.4 at.% T (T=Ni, Pd, Co, and Fe) in the respective phase diagrams.[17] The FLAPW band calculations described below were performed for the structure thus obtained for all T_2Zn_{11} (T=Ni, Pd, Co, and Fe) γ brasses by using the same parameters as those employed for the Cu_5Zn_8 and Cu_9Al_4 γ brasses.[16]

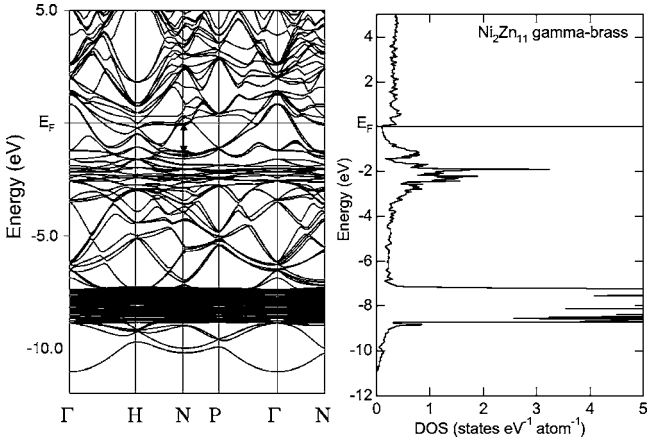

FIG. 2. *E-k* relations and the density of states for Ni_2Zn_{11} γ brass. A double-headed arrow marked at the point *N* in the dispersion relation indicates the position of the pseudogap.

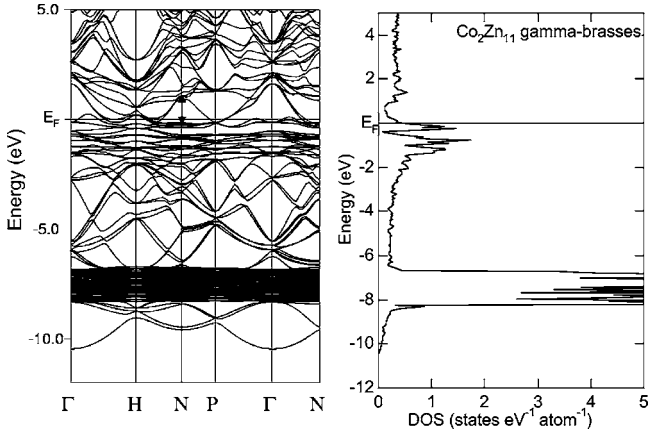

FIG. 4. *E-k* relations and the density of states for Co_2Zn_{11} γ brass. A double-headed arrow marked at the point *N* in the dispersion relation indicates the position of the pseudogap.

III. RESULTS AND DISCUSSION

A. Valence-band structure

The *E-k* relations and the density of states (DOS) were calculated for the Ni_2Zn_{11}, Pd_2Zn_{11}, Co_2Zn_{11}, and Fe_2Zn_{11} γ brasses by using the atomic structure described in Sec. II. The results are presented in Figs. 2–5. The center of the Zn-3*d* band is located at −7.5 to −8 eV for all four γ brasses, whereas that of the *T*-3*d* band is strongly *T*-species-dependent: −4.5, −2.5, −1, and −1 eV for *T* =Pd, Ni, Co, and Fe, respectively. This is compared with energies of −3.0 and −3.5 eV for Cu_5Zn_8 and Cu_9Al_4 γ brasses, respectively.[16] In the case of *T*=Pd, Ni, and Cu, the electronic structure very near E_F is the least affected by their 3*d* bands. In contrast, the Co- and Fe-3*d* states extend even above E_F and, hence, their effect on the electronic structure at E_F must be substantial.

The center and width of the pseudogap near E_F are determined from the gap states at the point *N* in the dispersion relation, as marked by a double-headed arrow in Figs. 2–5. The pseudogap is also seen as a trough in the DOS for all γ brasses studied. The same analysis was done for the Cu_5Zn_8 and Cu_9Al_4 previously studied.[16] The position of the pseudogap is shown in Fig. 6 with solid bars along with that for the *T*-3*d* band with open bars for all γ brasses studied. In the case of Cu_5Zn_8, Cu_9Al_4, and Pd_2Zn_{11}, the pseudogap appears well above the top of the *T*-*d* states so that it must be the least affected by the *d* band. It is also noteworthy that the pseudogap in these γ brasses is located either fully or partially below E_F. As mentioned in the Introduction, the electronic energy would be most effectively lowered when the pseudogap is partially filled such that E_F falls on the declining slope near its minimum like Cu_5Zn_8 and Cu_9Al_4. In the case of Ni_2Zn_{11}, the Ni-3*d* band exists immediately below the pseudogap and its effect on the pseudogap may not be ignored. But a gain in the electronic energy is certainly attained by the formation of the pseudogap, which is essentially fully submerged below E_F. Hence, we consider Ni_2Zn_{11} to be treated along the same line as Cu_5Zn_8, Cu_9Al_4, and Pd_2Zn_{11}.

A further careful look into Fig. 6 reveals a small shift toward a higher binding energy by about 0.5 eV in the position of the center of the pseudogap in both Ni_2Zn_{11} and

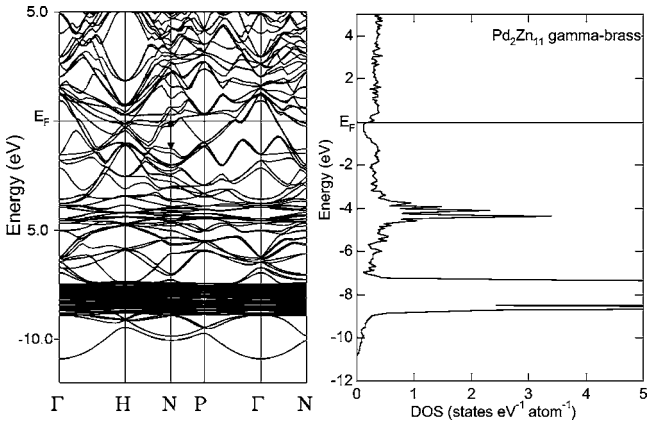

FIG. 3. *E-k* relations and the density of states for Pd_2Zn_{11} γ brass. A double-headed arrow marked at the point *N* in the dispersion relation indicates the position of the pseudogap.

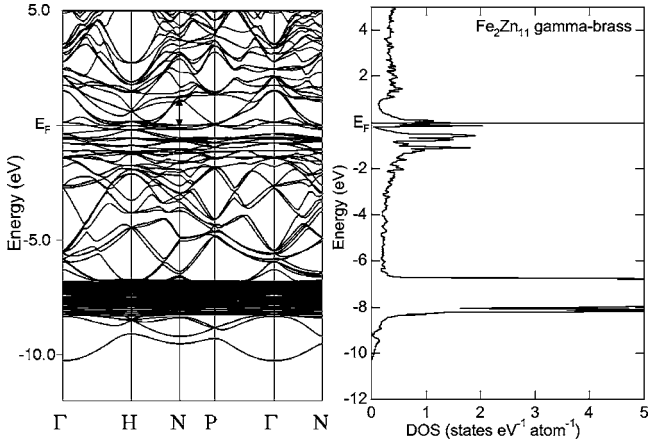

FIG. 5. *E-k* relations and the density of states for Fe_2Zn_{11} γ brass. A double-headed arrow marked at the point *N* in the dispersion relation indicates the position of the pseudogap.

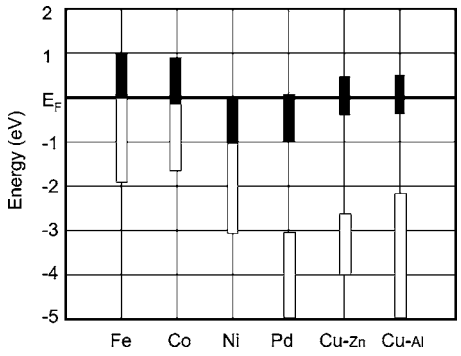

FIG. 6. Energy range where the pseudogap (solid bar) and the *T*-3*d* states (open bar) extend in Fe_2Zn_{11}, Co_2Zn_{11}, Ni_2Zn_{11}, Pd_2Zn_{11}, Cu_5Zn_8, and Cu_9Al_4 γ brasses. The data for the Cu_5Zn_8 and Cu_9Al_4 γ brasses were taken from Ref. 16.

Pd_2Zn_{11} γ brasses relative to that in the Cu_5Zn_8 and Cu_9Al_4. We noticed that the Zn-3*d* states in the former are centered at about −8.05 eV, which is again shifted by 0.5 eV toward higher binding energy than that in the latter. The same amount of the shift is also seen in the bottom of the valence band as well as the Zn-3*s* core level. This strongly indicates that the electrostatic potential of Zn ion is somewhat deeper in the Ni_2Zn_{11} and Pd_2Zn_{11} than in the remaining γ brasses and this is most likely responsible for the shift of the pseudogap. The total charge density in the muffin-tin potential around the Zn atom is calculated to see if there exists any difference between them. It turned out that the charge density is distributed around the value of 10.57–10.59 (wherein semicore 3*d* states dominate) without any distinctive difference among all the γ brasses studied, indicating that the difference in the electrostatic potential does not yield any sizable difference in the charge distribution around the Zn atom.

More significant is the finding of the pseudogap above E_F in the Co_2Zn_{11} and Fe_2Zn_{11} γ brasses. The pseudogap above E_F can no longer contribute to the stabilization of these γ brasses. More details will be discussed in connection with the resonance with the {330} and {411} zone planes in the following sections.

Before ending this section, it may be worthwhile to mention that atomic forces of ions turn out to be less than 10 mRy/a.u. and that further optimization or relaxation gave a negligible change in the band structure of the Fe_2Zn_{11} γ brass. This indicates that the structure we chose is fairly stable. A further test was made, since we are aware that the band structure and the Fourier analysis described below are sensitive to the choice of the structure. As mentioned above, there are two kinds of 8(c) sites, i.e., IT and OT in the 26-atom cluster in the γ structure. We performed the FLAPW band calculations for a "hypothetical" structure, in which *T* and Zn atoms are interchanged into IT and OT 8(c) sites, respectively. A rather large change in the band structure was observed. However, the structure showed a significant increase in the atomic forces, indicating that the hypothetical structure is unstable. By being encouraged from this test, we carried out the Fourier analysis below for the atomic structure described in Sec. II.

B. Fourier analysis of the FLAPW wave function

We direct our attention to the energy range near E_F in Figs. 2–5, where the pseudogap is formed. It was already emphasized that, among various symmetry points in Figs. 2–5, the effect of the Fermi surface–Brillouin zone interaction on the formation of the pseudogap is the most significant at the point *N* corresponding to the center of zone planes, for which two Miller indices are odd like {330} and {411}.[12,13] The square of the Fourier coefficient of the FLAPW wave function for a given band index *i* [see Eq. (1) in Ref. 16] in the energy range involving the pseudogap for the Cu_5Zn_8 and Cu_9Al_4 γ brasses was calculated at the point *N* in the reduced Brillouin zone and summed over equivalent zones.[16]

We say that the plane wave of $\mathbf{k}+\mathbf{G}=\mathbf{G}_{hkl}/2$ dominates in the FLAPW wave function when the magnitude of $\Sigma_{\{hkl\}}|C^i_{\mathbf{G}_{hkl}/2}|^2$ is extremely large at some particular set of the Miller indices (*hkl*). Indeed, the large value of $C^i_{\mathbf{k}+\mathbf{G}}$ was exclusively found, when $\mathbf{k}+\mathbf{G}$ coincides with one-half the reciprocal-lattice vectors corresponding to {330} and {411} planes, i.e., $\mathbf{k}+\mathbf{G}=\mathbf{G}_{330}/2$ and $\mathbf{k}+\mathbf{G}=\mathbf{G}_{411}/2$ in both Cu_5Zn_8 and Cu_9Al_4 γ brasses.[16] It was further revealed that the magnitude of $C^i_{\mathbf{G}_0/2}$ is almost the same as that of $C^i_{-\mathbf{G}_0/2}$ for every pair of $\mathbf{G}_0$, where the vectors $\mathbf{G}_{330}$ and $\mathbf{G}_{411}$ were collectively expressed as $\mathbf{G}_0$. A pairwise coupling between $\mathbf{G}_0/2$ and $-\mathbf{G}_0/2$ for electrons having the same energy eigenvalue near E_F certainly results in the formation of standing waves with the Fermi wave vector, i.e., either $\cos(\mathbf{k}_F\cdot\mathbf{r})$ or $\sin(\mathbf{k}_F\cdot\mathbf{r})$. This is merely the formation of the bonding and antibonding states across E_F due to the zone-boundary resonance effect associated with the planes {330} and {411}. This can be linked with a straightforward interpretation of the Hume-Rothery electron concentration rule from the first-principles band calculations.[16]

The Fourier coefficient $\Sigma_{\{hkl\}}|C^i_{\mathbf{G}_{hkl}/2}|^2$ for the present four γ brasses was now calculated from the FLAPW eigenfunction at the symmetry point *N* with an energy eigenvalue sustaining the pseudogap for the band with its index *i*. We revealed that $\Sigma_{\{hkl\}}|C^i_{\mathbf{G}_{hkl}/2}|^2$ is extremely large, when the square of the reciprocal-lattice vector $|\mathbf{G}|^2$ in the units of $(2\pi/a)^2$ or $h^2+k^2+l^2$ (hereafter abbreviated as Σh^2) becomes equal to 18, but that its magnitude is certainly dependent on the value of an energy eigenvalue chosen.

The Fourier coefficient $\Sigma_{\{hkl\}}|C^i_{\mathbf{G}_{hkl}/2}|^2$ thus obtained for the band *i* is plotted in Fig. 7 on the logarithmic scale as a function of Σh^2 for the four γ brasses studied. For instance, the largest one in the Pd_2Zn_{11} reaches 0.779 at $\Sigma h^2=18$ but the second largest one only 0.0251 at $\Sigma h^2=26$ corresponding to {510} and {431} zones, resulting in the intensity ratio of $I_{18}/I_{\text{next}}=31$. This clearly indicates that electrons at this energy exclusively resonate with {330} and {411} zones. Such intensive resonance with {330} and {411} zones is also observed in other γ brasses, though the intensity ratio I_{18}/I_{next} decreases from 28, 20, to 11 in the order of the Ni_2Zn_{11}, Co_2Zn_{11}, and Fe_2Zn_{11} at the energy shown in Fig. 7. Such a comparison should be made for electrons at different energy eigenvalues responsible for the formation of the pseudogap.

Figure 8 shows the energy dependence of the ratio of the Fourier coefficient of $\Sigma h^2=18$ over the second largest one,

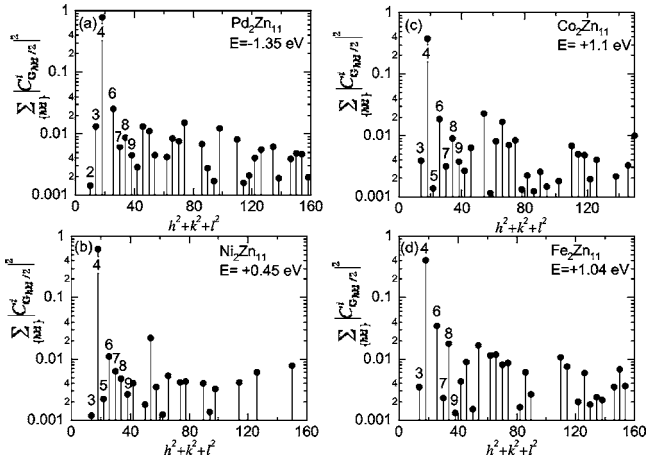

FIG. 7. The Fourier coefficient $\Sigma_{\{hkl\}}|C^i_{\mathbf{G}_{hkl}/2}|^2$ of the FLAPW wave function at the symmetry point N for the band i at the energy eigenvalue shown is plotted on the logarithmic scale as a function of Σh^2 for the four γ brasses studied. Major zone planes are numbered as follows: 2, {310}; 3, {321}; 4, {330}+{411}; 5, {332}; 6, {510}+{431}; 7, {521}; 8, {530}+{433}; 9, {611}+{532}.

I_{18}/I_{next}, for the present four γ brasses plus the Cu_5Zn_8 and Cu_9Al_4 previously studied. Let us first direct attention to the data for Cu_5Zn_8. The ratio is very large and reaches almost 40 over the range −0.62 to +0.68 eV, where the pseudogap is centered. In particular, the value exceeds 120 at −0.62 eV. This indicates that electrons at these energy eigenstates sharply resonate with the lattice periodicity due to {330} and {411} planes to form a standing wave totally in 36 directions, which, in turn, gives rise to the pseudogap as shown in Figs. 2–5. The resonance with {330} and {411} zones is no longer activated as the energy departs away beyond ±1 eV. The same is true for the Cu_9Al_4 γ brass: the ratio exceeds 20 over the range −0.5 to +0.5 eV, where the pseudogap exists.

In the Pd_2Zn_{11} and Ni_2Zn_{11} γ brasses, the ratio higher than 15 extends over the range −1.5 to +0.5 eV and −1.2 to +0.5 eV, in good agreement with the position of their pseudogap, respectively. In other words, the resonance of electron waves with the {330} and {411} lattice planes still predominates and, hence, must be responsible for the formation of the pseudogap below E_F in these γ brasses.

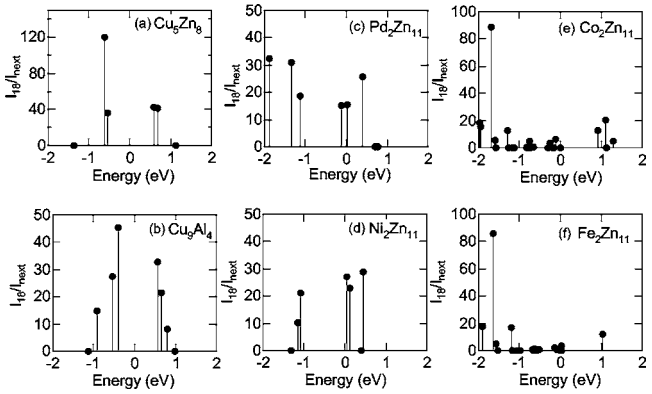

FIG. 8. Energy dependence of the ratio of the Fourier coefficient $I(=\Sigma_{\{hkl\}}|C^i_{\mathbf{G}_{hkl}/2}|^2)$ of the FLAPW wave function at $|\mathbf{G}_0|^2(=\Sigma h^2)=18$ over the next largest one, I_{18}/I_{next}, for the present four γ brasses plus the Cu_5Zn_8 and Cu_9Al_4 previously studied (Ref. 16). The value is distributed at lower- and higher-energy sides of the pseudogap in each case. An extremely large ratio is found at about $E=-1.5$ eV, well below the pseudogap in both Co_2Zn_{11} and Fe_2Zn_{11} γ brasses.

The situation is different in the Co_2Zn_{11} and Fe_2Zn_{11}. As remarked in Fig. 6, the pseudogap in these two γ brasses is located above E_F ranging up to $E=+1$ eV. The ratio I_{18}/I_{next} exceeding 10 appears at the higher energy side of the pseudogap. However, the ratio is substantially depressed at the lower energy side of the pseudogap or near E_F. This must be attributed to the admixture of the Co- and Fe-3d states, which apparently weakens the resonance with the zone planes. More surprising is the restoration of an extremely large value of the ratio exceeding 80 at about $E=-1.5$ eV for both γ brasses. There is indeed ample evidence for the formation of the pseudogap in the neighborhood of $E=-1.5$ eV, since the magnitude of $C^i_{\mathbf{G}_0/2}$ is confirmed to be almost the same as that of $C^i_{-\mathbf{G}_0/2}$ for every pair of $\mathbf{G}_0$, where $|\mathbf{G}_0|^2=18$. Nevertheless, there is no sign of the pseudogap in this energy range in their DOS, as can be seen in Figs. 4 and 5. This suggests that the effect of the T-3d states is small enough to restore a large ratio but still large enough to suppress the formation of the pseudogap due to the resonance with {330} and {411} zone planes at about $E=-1.5$ eV in both Co_2Zn_{11} and Fe_2Zn_{11} γ brasses.

C. Electronic structure constructed by averaging the wave vector having the largest Fourier component in the FLAPW wave function over the Brillouin zone

We pointed out in the preceding section that, as long as electronic states are not seriously perturbed by the d states at E_F, the plane wave $\mathbf{k}+\mathbf{G}$ giving rise to the largest Fourier component in the FLAPW wave function at the point N satisfies the condition $|\mathbf{G}_0|^2=18$ in the energy range involving the pseudogap near E_F. Encouraged by this finding, we now attempt to construct the electronic structure by averaging the wave vector $\mathbf{k}+\mathbf{G}$ of the plane wave having the largest Fourier expansion coefficient of the FLAPW wave function over a large number of selected electronic states in the Brillouin zone.

The value of $2(\mathbf{k}_i+\mathbf{G})$ giving the largest Fourier component was first deduced from the Fourier spectrum of the FLAPW wave function at a given energy eigenvalue for 200 special $\mathbf{k}_i$ points in the irreducible wedge corresponding to 1/48 of the reduced Brillouin zone.[26] The quantity $k_G(E)$ is defined as

$$k_G(E) \equiv \sum_{i=1}^{N} \omega_i |\mathbf{k}_i + \mathbf{G}|_E, \tag{1}$$

where i runs over the special $\mathbf{k}_i$ points, ω_i is a weight of the $\mathbf{k}_i$ point, and $|\mathbf{k}_i+\mathbf{G}|_E$ is evaluated at the energy E by linearly interpolating between energy eigenvalues. The weighting factor ω_i is the same as that for the DOS calculations. The square of the quantity given by Eq. (1), $\{2k_G(E)\}^2$, is now calculated as a function of energy for six γ brasses including Cu_5Zn_8 and Cu_9Al_4.

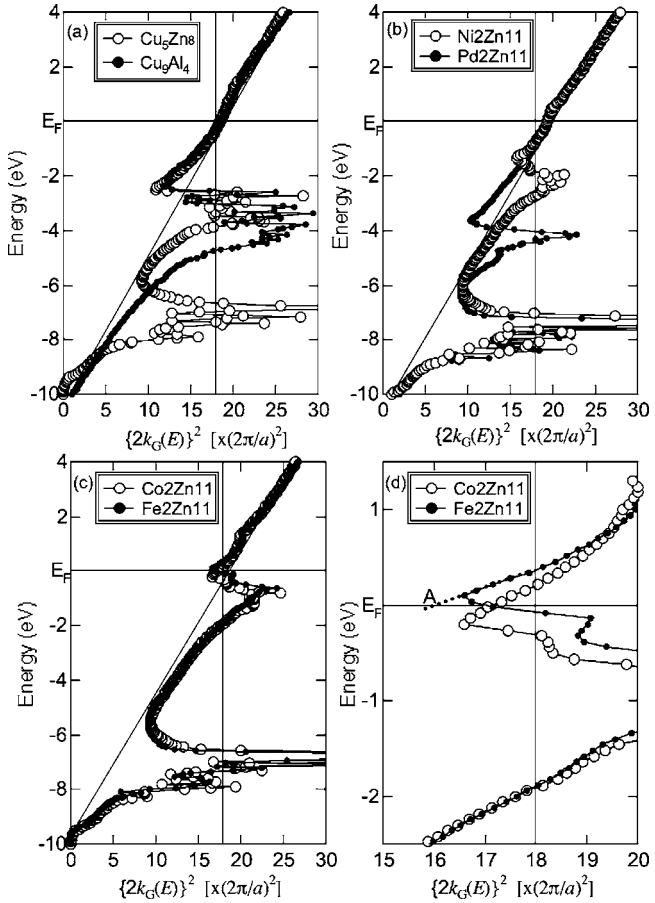

FIG. 9. The energy vs $\{2k_G(E)\}^2$ in units of $(2\pi/a)^2$, where a is the lattice constant, is plotted over the energy range −10 to +4 eV across E_F for (a) Cu_5Zn_8 and Cu_9Al_4, (b) Ni_2Zn_{11} and Pd_2Zn_{11}, and (c) Co_2Zn_{11} and Fe_2Zn_{11} γ brasses. The blow-up of (c) near E_F is reproduced in (d). The data for the Cu_5Zn_8 and Cu_9Al_4 γ brasses were taken from Ref. 16. The e/a for Fe in Fe_2Zn_{11} was determined from the intercept marked as "A" obtained by extrapolating the data above E_F as shown by a dotted line.

Before going into its details, we must note that $\{2k_G(E)\}^2$ is a quantity averaged over selected electronic states in the Brillouin zone. Hence, we consider it necessary to evaluate the degree of spreading around an averaged value. For this purpose, we introduce the standard deviation $\sigma(E)$ defined as

$$\sigma(E) = [2\{k_G(E) + \sigma_G(E)\}]^2 - \{2k_G(E)\}^2 = 8k_G(E)\sigma_G(E) + 4\sigma_G(E)^2, \quad (2)$$

where

$$\sigma_G(E) \equiv \sqrt{\sum_i \omega_i[|\mathbf{k}_i + \mathbf{G}|_E - k_G(E)]^2}. \quad (3)$$

We are now ready to investigate the energy dependence of $\{2k_G(E)\}^2$ while taking into account the value of σ given by Eqs. (2) and (3). The energy versus $\{2k_G(E)\}^2$ in the units of $(2\pi/a)^2$ for the three sets of γ brasses is plotted in Figs. 9(a)–9(c) over the energy range −10 to +4 eV. It happened that a very similar behavior is found for each set of γ brasses, i.e., (a) Cu_5Zn_8 and Cu_9Al_4, (b) Ni_2Zn_{11} and Pd_2Zn_{11}, and (c) Co_2Zn_{11} and Fe_2Zn_{11}. Correspondingly, the energy dependence of $\sigma(E)$ in units of $(2\pi/a)^2$ is shown in Figs. 10(a), 10(b), and 10(c).

The E versus $\{2k_G(E)\}^2$ relation may be regarded as a single-branch dispersion relation in the extended zone scheme for electrons represented by the dominant FLAPW wave function. Hence, it should fall on a straight line in the free-electron model. As is clearly seen from Fig. 9, the data calculated for a series of the γ brasses substantially deviate from the straight line in the energy range where d states exist. Two main peaks centered at −7 and −3 eV are certainly caused by the presence of Zn-3d and T-d states, respectively. A common background line can be drawn in Fig. 9 for all γ brasses except for the Ni_2Zn_{11} and Pd_2Zn_{11}, for which the line is apparently shifted by about 0.5 eV toward a higher binding energy in accord with the shift of the bottom of the valence band due to the difference in the electrostatic energy, as discussed earlier. Though the energy increases almost linearly with increasing $\{2k_G(E)\}^2$ well above E_F, a careful look into the data reveals that, after the termination of the T-d states, the energy always swings to a more positive direction or lower binding energy beyond the background straight line with a subsequent gradual approach to it. We see that the effect of the d states is essentially neglected at E_F in Cu_5Zn_8, Cu_9Al_4, Ni_2Zn_{11}, and Pd_2Zn_{11} but persists well above E_F in the case of Co_2Zn_{11} and Fe_2Zn_{11} γ brasses.

The dispersion curve in both Cu_5Zn_8 and Cu_9Al_4 crosses the $|\mathbf{G}|^2=18$ line at $E=-0.25$ eV near E_F. In addition, the $\sigma(E)$ shown in Fig. 10(a) is found to be very small in the energy range where the pseudogap exists across E_F. This is well consistent with our earlier conclusion that the $|\mathbf{G}_0|^2=18$ resonance occurs without being affected by the d states in this energy range. The $|\mathbf{G}|^2=18$ line crosses at $E=-0.8$ eV for both Pd_2Zn_{11} and Ni_2Zn_{11}, though their dispersion curves are still slightly below the background line. But, the $\sigma(E)$ shown in Fig. 10(b) is again well suppressed in the range $-1<E<0$ eV, where the pseudogap is formed. From this we say that the resonance with the {330} and {411} zone planes in both Pd_2Zn_{11} and Ni_2Zn_{11} is also not seriously affected by the T-d states to form the pseudogap immediately below E_F.

Now we discuss the dispersion relations and the corresponding $\sigma(E)$ for the Co_2Zn_{11} and Fe_2Zn_{11} γ brasses shown in Figs. 9(c) and 10(c). The data in both systems coincide well with each other, particularly above the T-d states. According to Fig. 9(d), their dispersion curves cross the $|\mathbf{G}|^2=18$ line three times at $E=-2.0$, -0.5 (or -0.2 in T=Co), and +0.5 eV. We revealed from Fig. 10(c) that the $\sigma(E)$ is substantially suppressed in the energy range $0.5<E<1$ eV and also near E=−2.0 eV. A small value of $\sigma(E)$ definitely supports that the $|\mathbf{G}_0|^2=18$ resonance does occur at these energy ranges. Instead, the value of $\sigma(E)$ in the vicinity of $E=-0.5$ eV (or -0.2 eV in T=Co), where $|\mathbf{G}|^2=18$ is also satisfied, is not as low as those mentioned above. This means that $|\mathbf{G}|^2=18$ at $E=-0.2$ or -0.5 eV is encountered simply as an average and has little to do with the resonance with {330} and {411} zones. This is quite consistent with our earlier argument based on Fig. 8.

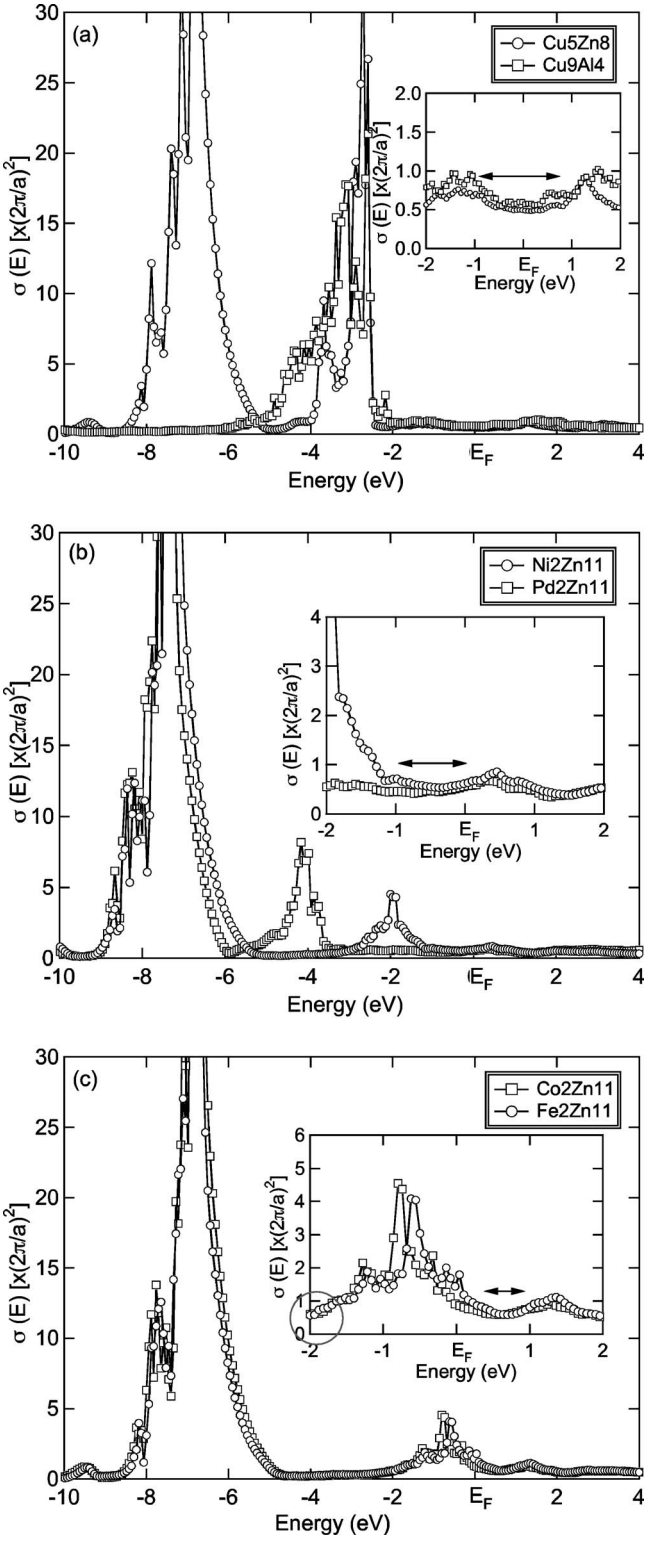

FIG. 10. Energy dependence of the standard deviation $\sigma(E)$ in the units of $(2\pi/a)^2$ defined by Eqs. (2) and (3) for (a) Cu_5Zn_8 and Cu_9Al_4, (b) Ni_2Zn_{11} and Pd_2Zn_{11}, and (c) Co_2Zn_{11} and Fe_2Zn_{11} γ brasses. The blow-up in the energy range, where the pseudogap is formed, is shown in the inset to each figure. The region near $E=-1.5$ to -2.0 eV in both Co_2Zn_{11} and Fe_2Zn_{11} is encircled to emphasize a substantial reduction in $\sigma(E)$. The region marked by a double-headed arrow in each inset refers to the position of the pseudogap.

TABLE I. e/a value and valency of T elements in the γ brasses. $\{2k_G(E)\}^2$ is in units of $(2\pi/a)^2$.

	E (eV) at $\{2k_G(E)\}^2=18$	$\{2k_G(E)\}^2$ at E_F	e/a	Valency of T element
Cu_5Zn_8	−0.28	18.47	1.599	0.96
Cu_9Al_4	−0.24	18.45	1.596	0.97
Ni_2Zn_{11}	−0.73	19.36	1.715	0.15
Pd_2Zn_{11}	−0.84	19.27	1.704	0.07
Co_2Zn_{11}	0.21	17.15	1.430	−1.7
Fe_2Zn_{11}	0.38	16.16	1.308	−2.5

D. Estimation of the effective e/a for γ brasses

The present FLAPW band calculations justified the use of the well-known Hume-Rothery electron concentration rule at least for the Cu_5Zn_8, Cu_9Al_4, Ni_2Zn_{11}, and Pd_2Zn_{11} γ brasses, for which the resonance with {330} and {411} zones is confirmed to occur at or immediately below E_F,

$$\left[\frac{3}{\pi}(e/a)N\right]^{2/3} = \Sigma h^2 = h^2 + k^2 + l^2 = 18, \tag{4}$$

where N is the number of atoms in the unit cell.[13]

Equation (4) may be applied to estimate the e/a value for Cu_5Zn_8, Cu_9Al_4, Pd_2Zn_{11}, and Ni_2Zn_{11}. An insertion of $N=52$ into Eq. (4) immediately leads to $e/a=1.538$, regardless of the constituent elements involved. This is obviously smaller than the magic number of 21/13. We consider the analysis based on Eq. (4) to be qualitatively correct but not to be quantitatively acceptable, since the electronic structure of individual systems is fully ignored. We consider it to be more important to estimate the e/a value for all T_2Zn_{11} γ brasses directly from the FLAPW band calculations.

The e/a value may be evaluated from the data in Fig. 9, since the value of $\{2k_G(E)\}^2$ at E_F would directly correspond to the square of the diameter of the Fermi sphere under the approximation that the plane wave $\mathbf{k}+\mathbf{G}$ dominates the FLAPW wave function outside the muffin-tin potential. The value can be easily read off from Fig. 9 for the Cu_5Zn_8, Cu_9Al_4, Ni_2Zn_{11}, and Pd_2Zn_{11} γ brasses. In the case of the Fe_2Zn_{11} and Co_2Zn_{11} γ brasses, however, it may not be legitimate to use directly the value at the intercept, since the dispersion below E_F is still under the intense influence of the T-d states. In other words, the dispersion relation shown in Fig. 9 is physically acceptable only in the region where the value of $\sigma(E)$ is sufficiently small. Thus, we determined the value at E_F by extrapolating the data above E_F where $\sigma(E)$ is small, as shown in Fig. 10(c). This is shown in Fig. 9(d).

Once the Fermi radius k_F is deduced, one can easily calculate the e/a value by using the relation $e/a=8\pi k_F^3/3N$, where k_F is in units of $2\pi/a$. The resulting e/a values for six γ brasses are listed in Table I. The valency of the T element is easily deduced by assuming valencies of Zn and Al to be 2 and 3, respectively. They are listed in the last column in Table I.

The e/a value is now system-dependent. In the case of Cu_5Zn_8, Cu_9Al_4, Ni_2Zn_{11}, and Pd_2Zn_{11}, the values become

closer to the magic number of 21/13(=1.615) than that of 1.538 derived from the oversimplified Hume-Rothery matching rule given by Eq. (4). The valency of Cu is found to be very close to unity for both Cu_5Zn_8 and Cu_9Al_4. This is in excellent agreement with the fact that Cu acts as a monovalent element in metallic state.

The valencies of Ni and Pd are deduced to be 0.15 and 0.07, respectively, both being fairly small positive values in contrast to the value of −0.6 proposed by Raynor.[18] As mentioned in the Introduction, Ekman[4] suggested that *T* atoms in the *T*-Zn (T=Ni, Pd, Co, Fe, etc.) γ brasses apparently contribute no electron to the valence band, i.e., a vanishing valency in order to force their electron concentration to meet the universal value of 21/13. We consider his idea to be roughly correct for *T*=Ni and Pd. In other words, we could theoretically confirm that the magic number of 21/13 is applicable not only to Cu_5Zn_8 and Cu_9Al_4 but also to Ni_2Zn_{11} and Pd_2Zn_{11}. However, this is not true for *T*=Co and Fe. The e/a values are much smaller than 21/13, indicating an apparent collapse of the universality of this magic number. The valencies for Co and Fe turn out to be −1.7 and −2.5, respectively, in good agreement with the values of −1.71 and −2.66 proposed by Raynor.[18] The possession of negative valencies for both Co and Fe certainly arises from the fact that the value of $\{2k_G(E)\}^2$ remains suppressed below the background level under the influence of the *T*-*d* states.

While admitting the presence of the neck in the Fermi surface of pure noble metals as established in the late 1950s, Hume-Rothery mentioned in 1961 that the stability of noble metal alloys is better described in terms of a spherical Fermi surface touching the relevant Brillouin zones.[27] According to the present analysis based on the FLAPW band calculations, we could reasonably construct a Fermi sphere for all γ brasses studied. The spherical Fermi surface thus constructed has little to do with a real one but, we believe, is essentially the same notion as that Hume-Rothery intuitively assumed in 1961. In other words, the Hume-Rothery electron concentration rule $2k_F=K_p$ can be more rigorously discussed in terms of the Fermi sphere constructed from dominant plane waves in the Fourier expansion of the FLAPW wave function.

E. Stability of the γ-brass phase

The present analysis so far discussed led us to conclude that the stability of the Cu_5Zn_8, Cu_9Al_4, Ni_2Zn_{11}, and Pd_2Zn_{11} γ brasses is brought about by the pseudogap across E_F. Its origin was well accounted for in terms of resonance of electrons having the highest kinetic energies with the {330} and {411} zones. We believe that the present first-principles band calculations afford a sound basis for the interpretation of the Hume-Rothery electron concentration rule regarding why the γ-brass structure is stabilized at a particular electron concentration equal to 21/13.

In the case of the Co_2Zn_{11} and Fe_2Zn_{11} γ brasses, the pseudogap is revealed in unoccupied DOS above E_F. This obviously means no gain in the electronic energy by the formation of the pseudogap. However, a detailed analysis in Sec. III C allowed us to conclude that intense resonance with the {330} and {411} zones is occurring at about $E=-1.5$ eV in both cases. A pairwise coupling between $\mathbf{G}_0/2$ and $-\mathbf{G}_0/2$ is also confirmed. This will naturally result in the formation of cos- and sin-type standing waves and thereby the split of the band into bonding and antibonding states separated by a pseudogap. But, there is no pseudogap in the range centered at $E=-1.5$ eV in the respective DOS in Figs. 4 and 5. It may be masked by the superimposed *T*-3*d* states. We consider the masked resonance still to contribute to gaining the electronic energy relative to the case in which it is missing.

According to the phase diagram, both Co-Zn and Fe-Zn γ brasses exist as a single phase over the composition range 15–35 at.% Co and 15–31 at.% Fe, respectively. The present band calculations were performed only at the minimum *T* concentration of T_2Zn_{11} or 15.3 at.% *T* to avoid chemical disorder in atomic sites 8(c). It is still premature to pursue the first-principles band calculations to explore why nature selects more favorably the *T*-richer γ-brass structure by introducing chemical disorder into the T_2Zn_{11}. A closer inspection into the DOS in the Fe_2Zn_{11} and Co_2Zn_{11} γ brasses in Figs. 4 and 5 reveals the presence of a sharp gap at about 0.5 eV below E_F. If the total electron concentration is decreased by increasing the *T* concentration at the expense of Zn, the Fermi level would be trapped into the bottom of this gap, leading to the stabilization of the γ-phase structure. We performed the LMTO-ASA band calculations for this purpose. The DOS shown in Figs. 4 and 5 is well reproduced. The gap was proven to originate from splitting into bonding and antibonding states due to the orbital hybridizations between the Fe-3*d* and Zn-4*sp* states. Further work is challenging to specify the stability mechanism for Co-Zn and Fe-Zn γ brasses, particularly, if possible, by taking into account the chemical disorder in the lattice.

IV. CONCLUSION

The FLAPW band calculations for a series of T_2Zn_{11} (*T*=Ni, Pd, Co, and Fe) γ brasses revealed that electrons near E_F resonate with the {330} and {411} zone planes and give rise to the pseudogap in the same way as in the Cu_5Zn_8 and Cu_9Al_4 γ brasses reported earlier.[16] The pseudogap is formed below E_F in Cu_5Zn_8 and Cu_9Al_4 and T_2Zn_{11} (*T*=Ni and Pd) but essentially above it in T_2Zn_{11} (T=Co and Fe). The phase stability was successfully discussed in terms of the Fermi surface–Brillouin zone interaction in the former. The resonance with the {330} and {411} zones as well as Zn-4*sp*/Co- or Fe-3*d* orbital hybridizations is suggested to be of importance in the latter. The e/a value is determined for all six γ brasses by constructing a single-branch energy dispersion relation in the extended zone scheme. The e/a value thus obtained is found to be close to 21/13=1.615 for Cu_5Zn_8, Cu_9Al_4, Ni_2Zn_{11}, and Pd_2Zn_{11} γ brasses but to be only 1.4 and 1.3 for Co_2Zn_{11} and Fe_2Zn_{11}, respectively. The present study could provide a theoretical basis for the Hume-Rothery electron concentration rule for Cu_5Zn_8, Cu_9Al_4, Ni_2Zn_{11}, and Pd_2Zn_{11} γ brasses from the first-principles band calculations. Further elaboration is needed for Co-Zn and Fe-Zn γ brasses, particularly by taking into account the role of chemical disorder.

*Present address: Toyota Physical & Chemical Research Institute, Nagakute, Aichi 480-1192, Japan.

[1] A. J. Bradley and J. Thewlis, Proc. R. Soc. London, Ser. A **112**, 678 (1926).

[2] A. Westgren and G. Phragmén, Metallwirtschaft **7**, 700 (1928).

[3] A. F. Westgren and G. Phragmén, Trans. Faraday Soc. **25**, 379 (1929).

[4] W. Ekman, Z. Phys. Chem. Abt. B **12**, 57 (1931).

[5] N. F. Mott and H. Jones, *The Theory of the Properties of Metals and Alloys* (Clarendon Press, Oxford, England, 1936), pp. 168–174

[6] A. P. Tsai, A. Inoue, and T. Masumoto, Jpn. J. Appl. Phys., Part 2 **27**, L1587 (1988); A. P. Tsai, A. Inoue, Y. Yokoyama, and T. Masumoto, Mater. Trans., JIM **31**, 98 (1990).

[7] Y. Yokoyama, A. P. Tsai, A. Inoue, T. Masumoto, and H. S. Chen, Mater. Trans., JIM **32**, 421 (1991).

[8] T. Fujiwara, Phys. Rev. B **40**, 942 (1989).

[9] J. Hafner and M. Krajcí, Phys. Rev. B **47**, 11795 (1993).

[10] M. Windisch, M. Krajci, and J. Hafner, J. Phys.: Condens. Matter **6**, 6977 (1994).

[11] G. Trambly de Laissardiére and T. Fujiwara, Phys. Rev. B **50**, 5999 (1994).

[12] H. Sato, T. Takeuchi, and U. Mizutani, Phys. Rev. B **64**, 094207 (2001).

[13] H. Sato, T. Takeuchi, and U. Mizutani, Phys. Rev. B **70**, 024210 (2004).

[14] E. Belin-Ferré, J. Phys.: Condens. Matter **14**, R789 (2002).

[15] Z. M. Stadnik, D. Purdie, M. Garnier, Y. Baer, A.-P. Tsai, A. Inoue, K. Edagawa, S. Takeuchi, and K. H. J. Buschow, Phys. Rev. B **55**, 10938 (1997).

[16] R. Asahi, H. Sato, T. Takeuchi, and U. Mizutani, Phys. Rev. B **71**, 165103 (2005).

[17] H. Okamoto, *Phase Diagrams for Binary Alloys* (ASM International, Metals Park, OH, 2000).

[18] G. V. Raynor, Prog. Met. Phys. **1**, 1 (1949).

[19] J. B. Haworth and W. Hume-Rothery, Philos. Mag. **43**, 613 (1952).

[20] G. Trambly de Laissardiére, D. N. Manh, L. Magaud, J. P. Julien, F. Cyrot-Lackmann, and D. Mayou, Phys. Rev. B **52**, 7920 (1995)

[21] *Pearson's Handbook*, edited by P. Villars (ASM International, Materials Park, OH, 1997), Vol. 2.

[22] U. Mizutani, T. Takeuchi, K. Saito, and N. Tanaka, The convergent beam electron diffraction studies coupled with the Rietveld structure analysis for powered diffraction spectrum measured at Synchrotron radiation facility, SPring-8, Japan, were consistent with the possession of $I\bar{4}3m$ for the $Co_{20}Zn_{80}$ γ brass. In the best refined structure, chemical disorder is present only in IT and OT sites 8(c) with the lattice constant of 8.8568 Å.

[23] A. Johansson, H. Ljung, and S. Westman, Acta Chem. Scand. (1947-1973) **22**, 2743 (1968).

[24] V.-A. Edström and S. Westman, Acta Chem. Scand. (1947-1973) **23**, 279 (1969).

[25] J. K. Brandon, R. Y. Brizard, P. C. Chieh, R. K. McMillan, and W. B. Pearson, Acta Crystallogr., Sect. B: Struct. Crystallogr. Cryst. Chem. **30**, 1412 (1974).

[26] H. J. Monkhorst and J. D. Pack, Phys. Rev. B **13**, 5188 (1976).

[27] W. Hume-Rothery, J. Inst. Met. **9**, 42 (1961).